GCM Tests of Theories for the Height of the Tropopause

JOHN THUBURN

Centre for Global Atmospheric Modelling, Department of Meteorology, University of Reading, Reading, United Kingdom

GEORGE C. CRAIG

Joint Centre for Mesoscale Meteorology, Department of Meteorology, University of Reading, Reading, United Kingdom

(Manuscript received 21 March 1996, in final form 16 September 1996)

ABSTRACT

The sensitivity of the tropopause height to various external parameters has been investigated using a global circulation model (GCM). The tropopause height was found to be strongly sensitive to the temperature at the earth's surface, less sensitive to the ozone distribution, and hardly sensitive at all to moderate changes in the earth's rotation rate. The strong sensitivity to surface temperature occurs through changes in the atmospheric moisture distribution and its resulting radiative effects. The radiative and dynamical mechanisms thought to maintain the tropopause height have been investigated in some detail. The assumption that the lower stratosphere is close to radiative equilibrium leads to an easily computed relationship between tropospheric lapse rate and tropopause height. This relationship was found to hold well in the GCM in the extratropics away from the winter pole. Possible reasons for the breakdown of the relationship in the Tropics and near the winter pole are discussed. Simple relationships predicted by two different baroclinic adjustment theories, between parameters such as potential temperature gradients, the Coriolis parameter, and tropopause height, were examined. When some of these parameters were changed explicitly in GCM experiments, the remaining parameters, determined internally by the GCM, did not respond in the predicted way. These results cast doubt on the relevance of baroclinic adjustment to the height of the tropopause.

1. Introduction

The tropopause is one of the most basic features of the temperature structure of the earth's atmosphere. Despite this, it is still not clearly understood what determines the height of the tropopause, why it is so sharp in places, and even why it exists at all. This is an important gap in our understanding of the general circulation. In addition, the question of what maintains the structure of the tropopause is intimately related to the question of the mechanisms and rates of exchange of air, moisture, and trace chemicals between the troposphere and the stratosphere, which has implications for the chemistry of both the troposphere and the stratosphere (e.g., Holton et al. 1995).

A useful working definition of the tropopause is in terms of the lapse rate (e.g., Lewis 1991): ''The tropopause is the lowest level at which the lapse rate decreases to 2°C km^{-1} or less, provided also that the average lapse rate between this level and all higher levels within 2 km does not exceed 2°C km^{-1}.'' Alternative definitions have been proposed, for example, in terms of isosurfaces of Rossby–Ertel potential vorticity (PV). However, different authors advocate the use of different PV isosurfaces (e.g., Hoerling et al. 1991), and there exists a whole family of PV-like quantities whose use is no less justifiable theoretically than the use of PV itself (Lait 1994), but whose isosurfaces do not coincide with PV isosurfaces. The justification for using these definitions appears to be that, to a good approximation, the tropopause is a material surface over timescales of a few days, plus, of course, the near coincidence of the PV tropopause with the lapse rate tropopause. In this paper we take the point of view that the observed tropopause is primarily a feature of the temperature structure, and therefore we use the lapse-rate definition. If a successful explanation for this temperature structure can be found then this may suggest a more appropriate definition. For example, if isentropic mixing of PV in the troposphere can be shown to play an important role in sharpening the extratropical tropopause, as suggested by McIntyre and Palmer (1984), then a definition of the tropopause based on isentropic gradients of PV may be most appropriate in the extratropics.

In reality the tropopause can have quite a complicated structure. There may be sharp steps at the polar front and subtropical front, there may be several levels at

Corresponding author address: Dr. John Thuburn, CGAM, Dept. of Meteorology, University of Reading, 2 Earley Gate, Whiteknights, Reading RG6 2AU, United Kingdom.
E-mail: swsthubn@met.rdg.ac.uk

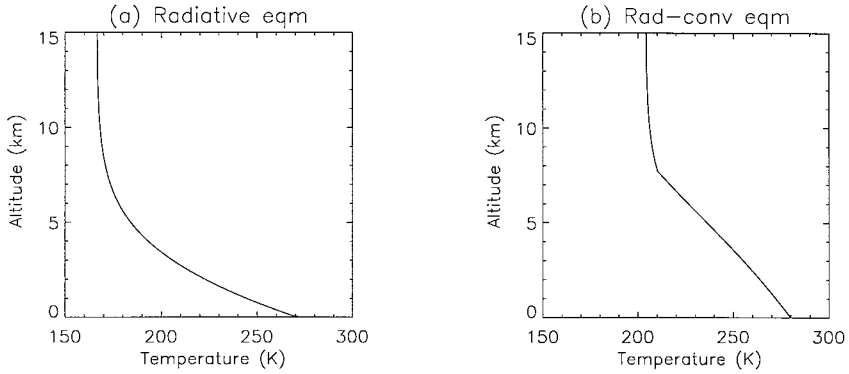

FIG. 1. (a) Radiative equilibrium temperature profile; (b) radiative–convective equilibrium temperature profile.

which the lapse rate definition is satisfied, and there may exist ''tropopause folds'' associated with jet streams and synoptic systems in midlatitudes (e.g., Palmén and Newton 1969; Shapiro et al. 1987). This investigation will consider only the zonal mean structure of the atmosphere over a timescale of a few weeks, for which the height of the tropopause can be considered steady.

The simplest explanation for the existence of the tropopause is in terms of a radiative–convective model (e.g., Houghton 1977). Consider an atmosphere that does not absorb solar radiation, so that it is heated from below by the ground but is radiatively active with respect to thermal infrared radiation. For earthlike parameters, the radiative equilibrium temperature profile for such an atmosphere decreases very rapidly with height near the ground and, in fact, is statically unstable there (Fig. 1a). It is assumed, then, that the temperature profile near the ground is adjusted by convective overturning to a statically neutral state (a moist adiabat when moisture is taken into account), while at higher levels a radiative equilibrium profile, which is statically stable, is maintained (Fig. 1b). The resulting temperature profile has a sharp change in gradient at the top of the convectively adjusted layer, which has been identified with the tropopause.

While this simple model represents a plausible explanation for the tropical tropopause, it cannot explain the observed structure in other regions. Most obviously, the lapse rate in the extratropical troposphere (typically 4.5–5.5 K km^{-1}) is generally more stable than a moist adiabat (about 8–9 K km^{-1}), suggesting that it is determined by some process other than moist convection. Several authors have suggested that baroclinic adjustment might play a role in determining the temperature structure of the extratropical troposphere and hence in determining the height of the extratropical tropopause. Baroclinic adjustment implies that when large-scale forcing tends to make the mean atmospheric state baroclinically unstable, the effect of the resulting baroclinic eddies is to maintain the mean state close to neutral stability. The assumption of baroclinic adjustment can be regarded as a parameterization of the effects of baroclinic eddies. The structure of the baroclinically neutral state may provide an alternative constraint on the tropospheric lapse rate or tropopause height.

A useful conceptual separation of the roles of radiation and dynamics was introduced by Held (1982). Given a tropospheric lapse rate, whatever maintains it, the assumption that the lower stratosphere is in radiative equilibrium makes it possible to calculate a tropopause height. The radiative equilibrium assumption thus leads to a functional relationship between the tropospheric lapse rate γ and the tropopause height H, which may be referred to as the *radiative constraint.* In the Tropics γ is presumed to be determined by moist convective adjustment, and hence H is determined. In the extratropics a baroclinic adjustment theory that gives a second relationship between γ and H again implies that both γ and H are determined. Such a relationship, obtained from convective or baroclinic adjustment, represents a *dynamical constraint.*

Held derived a quantitative version of the radiative constraint using a very simple gray-atmosphere model to obtain a relationship between lapse rate and tropopause height. In order to close the problem it is necessary to specify the optical depth τ as a function of height (determined by atmospheric composition, see section 4 below) and a boundary condition such as outgoing longwave radiation at the top of the atmosphere, or surface temperature T_*. As discussed in section 4, the surface temperature condition will be employed in this paper. The radiative constraint can then be depicted schematically as

$$H = H_{\mathrm{RAD}}(T_*, \gamma, \tau). \tag{1}$$

Although Held (1982) used a very simple model, the calculation could be made more precise using a more sophisticated radiative transfer code.

A quantitative expression of the dynamical constraint from baroclinic adjustment requires a description of the baroclinically neutral state in which the atmosphere is

assumed to be found. For a two-layer model the stability boundary is given by

$$\bar{T}_y = -H_{(\rho)} \frac{\beta}{f} \bar{\theta}_z \tag{2}$$

(Phillips 1954; Stone 1978). Here an overbar indicates a zonal mean, T is the temperature at the interface between the two layers, θ_z is the vertical gradient of potential temperature between the two layers, f is the Coriolis parameter and β its northward gradient, and $H_{(\rho)} = RT/g$ is a density scale height, where R is the gas constant for air and g is the acceleration due to gravity. Stone (1978) presented evidence that the observed midlatitude midtropospheric meridional temperature gradient resembles that predicted by (2), and Stone and Carlson (1979) presented evidence that the observed midlatitude tropospheric lapse rate resembles that predicted by (2).

The stability condition found for the two-layer model is an example of a more general condition. Under quasigeostrophic scaling, sufficient conditions for stability are that the zonal-mean northward gradient of the quasigeostrophic PV $\bar{q}_y$ be greater than or equal to zero and that $\bar{\theta}_y$ at the ground be greater than or equal to zero (Charney and Stern 1962). When relative vorticity is neglected, the condition that $\bar{q}_y$ should vanish becomes

$$\beta + \frac{f}{\rho}\left(\rho \frac{\bar{\theta}_y}{\bar{\theta}_z}\right)_z = 0. \tag{3}$$

This suggests a relationship of the form

$$\bar{\theta}_y \approx -H_{(s)} \frac{\beta}{f} \bar{\theta}_z, \tag{4}$$

which closely resembles (2), although in this case the interpretation of the height scale $H_{(s)}$ is less obvious.

Held (1982) argued that the height scale in Eq. (4) could be interpreted as the depth over which baroclinic eddies can effectively transport heat and therefore should define the depth scale that determines the height of the tropopause. In particular, following Lindzen and Farrell (1980b), he calculated the depth over which the vertical shear (or, equivalently, $\bar{\theta}_y$) must be adjusted, given $\bar{\theta}_z$, in order to eliminate regions of negative $\bar{q}_y$ and surface $\bar{\theta}_y$. This gave an expression similar to (4) for the dynamical constraint. He found that this, in combination with his radiative constraint, gave a plausible estimate of the height of the extratropical tropopause.

Gutowski (1985), however, claimed that the temperature profile that results from this adjustment does not resemble the observed profile, and the adjustment to a neutral state must occur in another way. Instead he proposed that $\bar{\theta}_z$ is adjusted, given $\bar{\theta}_y$, so as to eliminate regions of negative $\bar{q}_y$. In this case it is not possible to eliminate negative $\bar{\theta}_y$ at the ground, but the mean flow can be ''effectively'' stabilized in the sense that only shallow waves, which are inefficient at transporting heat, remain unstable. Although the way that the temperature field adjusts is different from that described by Held (1982), the relationship between $\bar{\theta}_y$, $\bar{\theta}_z$, and $H_{(s)}$ in the adjusted state implied by (4) remains the same.

A fundamentally different description of the baroclinically neutral state was provided by Lindzen (1993), who suggested that the mean flow can be stabilized without eliminating regions of negative $\bar{\theta}_y$ at the ground. He considered the Eady (1949) model of baroclinic instability to be most relevant in view of the weak PV gradients that exist in the troposphere and the strong gradients at the tropopause. In this model all unstable modes have a total horizontal wavenumber K less than $K_{\max}$ given by

$$K_{\max}^2 = (2.3394)^2 \frac{f^2}{N^2 H^2}. \tag{5}$$

At the same time the finite jet width precludes unstable modes with K less than some $K_{\min}$. The baroclinic adjustment hypothesis in this case is that baroclinic eddies modify N^2 and H, and possibly the jet width, until $K_{\max} = K_{\min}$, thereby neutralizing the mean state. Thus, according to this theory, H depends on f, N^2, and the jet width through (5). Consequently, the expected response of H to changes in external parameters like the planet's rotation rate depends on whether the jet width is controlled essentially by the scale of the planet or by some property of the flow like the Rhines (1975) β-scale.

Egger (1995) has examined the effect of Eady-type instabilities on the mean state over the course of unstable wave life cycles using a β-plane channel model. He found that the unstable waves tend to stabilize the mean state, primarily by modifying N rather than H. However, it is not clear how these results relate to the long term balance between forcing of the mean state and eddy feedbacks in the climate context.

It is not only the description of the baroclinic adjustment process that is uncertain, but also whether it is reasonable to expect the atmosphere to be in an adjusted state at all. As shown for example by Valdes and Hoskins (1988), the zonal mean state of the atmosphere is unstable to growing baroclinic waves. In a simpler context, Vallis (1988) and Stone and Branscome (1992) have investigated whether baroclinic adjustment occurs in fully nonlinear two-layer models. Both studies found that a statistical equilibrium could be attained in which the mean shear was significantly greater than the critical shear. However, in the cases studied by Stone and Branscome the equilibrated shear was, to a good approximation, a constant multiple of the critical shear over a range of parameter space. If such a relationship were found to hold for the real atmosphere it would still be useful as a basis for a parameterization of the effects of baroclinic eddies. Stone and Branscome call this ''weak baroclinic adjustment.''

The theories of baroclinic adjustment discussed here all involve vanishing, or at least relatively small, meridional PV gradients in the troposphere. Indeed, wheth-

er or not the atmosphere approaches a baroclinically neutral state, eddies will tend to mix PV and so eliminate its gradients. Sun and Lindzen (1994) have examined the implications for the tropospheric temperature and wind structure of assuming Rossby–Ertel PV to be well mixed along isentropes. The possible role of PV mixing in sharpening the tropopause has been suggested by McIntyre and Palmer (1984). Note, however, that the assumption that meridional PV gradients vanish is insufficient, on its own, to determine the temperature structure. In addition one must assume, for example, that $\bar{\theta}_z$ is given (e.g., Held 1982), or that $\bar{\theta}_y$ is given (e.g., Gutowski 1985), or that PV is a given function of $\bar{\theta}$ (e.g., Sun and Lindzen 1994).

The most straightforward way of testing the formulas (2), (4), or (5) predicted by baroclinic adjustment theory is to show that the formulas hold, at least approximately, when observed values of the relevant parameters are inserted (Stone 1978; Held 1982; Lindzen 1993). Similar comments apply to the radiative constraint (1) discussed by Held (1982). All the theories discussed here have produced plausible results. A stronger test is to examine whether the parameters in these formulas vary together in the predicted way; in other words, to determine whether the height of the tropopause scales according to these relationships. Such a test is not necessarily feasible using observed data because the observed atmospheric state occupies only a small part of the parameter space. However, it is feasible using a numerical model of the atmosphere.

This paper describes the results of a set of GCM experiments designed to provide such a test of these radiative and dynamical relationships. External parameters and boundary conditions of the GCM have been varied in such a way as to cause significant variations in as many as possible of the parameters in the radiative and dynamical relationships, and the results are compared to the theoretical predictions. These experiments are described in section 2. The variation of H with surface temperature and lapse rate predicted by the radiative constraint is examined in section 4. The variation of parameters in formulas (4) and (5) predicted by baroclinic adjustment theory is examined in section 5. The conclusions are summarized in section 6.

2. Model and experimental design

The model used for these experiments is a version of the U.K. Universities Global Atmospheric Modelling Programme (UGAMP) GCM (e.g., Slingo et al. 1994). It is a spectral model, here run at T42 horizontal resolution, and includes representations of radiative transfer (Morcrette 1990), moist processes including deep and shallow convection (Betts and Miller 1994), and large-scale condensation, boundary layer processes, orographic gravity wave drag, and surface processes. The main difference between the version used here and the version described by Slingo et al. is that the number of vertical levels is increased from 19 to 33, providing increased vertical resolution in the region of the tropopause (Fig. 2). In addition, a less diffusive shape-preserving scheme, based on fourth order differences plus Leonard's (1991) universal limiter, is used for vertical advection. A specified ozone distribution (Shine 1989) is used for the radiative heating calculations.

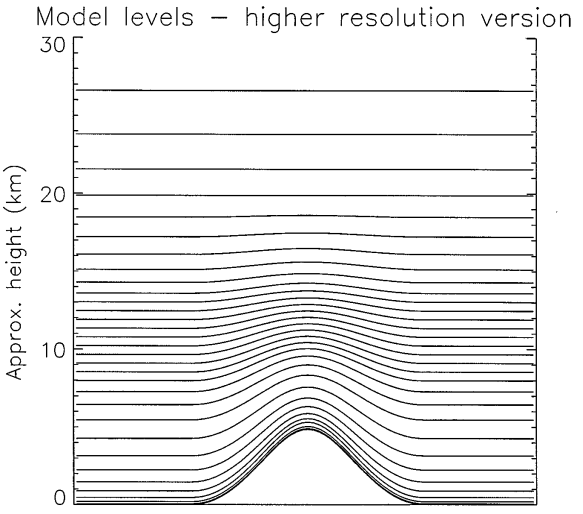

FIG. 2. Locations of the UGAMP GCM levels, showing how they deform over a typical mountain to remain terrain following. Note the enhanced vertical resolution around the tropopause used in the experiments in this paper.

In this version of the UGAMP GCM the sea surface temperature and the deep soil temperature (i.e., the temperature in the lowest layer of a three-layer soil model) are specified. The surface soil temperature is relaxed towards the specified deep soil temperature on a timescale of order 3 days so that, on timescales longer than this, the surface temperature can be considered to be effectively imposed over land as well as sea. Therefore, in these experiments, the surface temperature is part of the given boundary conditions and does not respond to changes in other forcing parameters. Some of the experiments described below test the sensitivity of the tropopause height to changes in forcing parameters other than surface temperature. It should be remembered that these sensitivities are for fixed surface temperature. If the surface temperature were internally determined by the system and allowed to respond to changes in forcing, as it would be in the real world or in a more complete GCM, the sensitivity of the tropopause height to changes in forcing could be quite different after the surface temperature eventually adjusts to a new equilibrium. However, this adustment to equilibrium will be dominated by the very long timescale response of the oceans; on much shorter timescales the sensitivity of the tropopause height would be similar to that for fixed sea surface temperature.

A control experiment was run using the standard model configuration for 120 days with ''perpetual January''

TABLE 1. Summary of the GCM experiments carried out.

Experiment number	Description	Parameters explicitly perturbed
1	Control	
2	Ozone concentration shifted downward one scale height	
3	Ozone removed	
4	Planet's rotation rate increased by 40%	f, β
5	Planet's rotation rate decreased by 40%	f, β
6	Lower boundary temperature reduced uniformly by 10 K	T_*
7	Lower boundary temperature reduced uniformly by 20 K	T_*
8	Lower boundary temperature reduced by (20 K)$\sin^2\phi$	T_*, $\bar{\theta}_y$
9	Lower boundary temperature increased by (20 K)$\sin^2\phi$	T_*, $\bar{\theta}_y$
10	Perpetual July	

solar forcing, sea surface temperatures, and deep soil temperatures and moistures. Perpetual solstice forcing was chosen because it was not clear, before running these experiments, how quickly the state of the atmosphere would respond to changes in forcing. In practice, we found that the model atmosphere responded to the changes in forcing described below on a timescale of about 2–4 weeks. This suggests that our conclusions would remain valid if annual cycle forcing were used instead.

In constructing perturbation experiments, the first issue is to identify which of the parameters in (1), (4), and (5) are imposed externally and can be varied explicitly, and which are determined internally by the model. Clearly f, β, and, as discussed above, surface temperature T_* are externally specified, while tropopause height H and static stability $\bar{\theta}_z$ are determined internally. The meridional temperature gradient $\bar{\theta}_y$ is partly determined by the dynamics but is strongly influenced by the imposed surface temperature gradient. Similarly the optical depth, which is dominated by water vapor in the long wave, will be determined internally but will be strongly influenced by the imposed surface temperatures.

In determining the magnitude of the perturbations, two conflicting requirements must be satisfied. First, the changes must be large enough to measurably affect the tropopause height. Second, they must not be so large as to perturb the climate into another regime where the structure of the atmosphere is controlled by different processes. A simple example of an unacceptable perturbation would be to set the rotation rate of the planet to zero. In this case the Hadley circulation would extend to the pole (Williams and Holloway 1982), and there is little reason to expect baroclinic adjustment to be of any relevance to the resulting state.

Nine further experiments were run, again for 120 days, as summarized in Table 1 and described in detail in the following paragraphs. The absorption of solar radiation by ozone is important for maintaining the very stable stratification of the stratosphere and might be expected to play a role in determining the tropopause height. However, this ozone heating is neglected in the simple radiative model used by Held (1982) and in section 4 below to derive the radiative constraint. To assess the importance of ozone in determining tropopause height, two experiments were performed in which the ozone distribution was changed. In the first, the profile of ozone concentration was shifted downward by one pressure scale height (approximately 7 km) while maintaining the same total column amount. In the second, the ozone was removed completely. An additional reason for carrying out these experiments is to rule out the possibility that the GCM tropopause may be artificially constrained by the use of a fixed climatological ozone distribution rather than a more realistic interactive one.

The baroclinic adjustment theories described by (2) and (4) suggest that the mean isentropic slope, and hence the tropopause height, should be insensitive to the planet's rotation rate. However, the adjustment mechanism proposed by Lindzen (1993) could lead to a dependence of tropopause height on the planet's rotation rate, depending on what controls the jet width and the scale of the eddies. Two experiments were performed in which the planet's rotation rate, as it affects the Coriolis parameter, was changed, either increased by 40% or decreased by 40%. (However, the length of day was not changed.) The planet was spun up or spun down over the first 15 days of each experiment. These experiments test the null result predicted by (2) and (4) and could provide a way of distinguishing between the different baroclinic adjustment mechanisms.

The moist adiabatic lapse rate depends on the surface temperature, so the tropical tropopause height is expected to depend on surface temperature. Also, the radiative relationship described in section 4 predicts a strong dependence of tropopause height on surface temperature even for a given lapse rate. The baroclinic adjustment theories, on the other hand, predict no direct dependence of tropopause height on surface temperature, although the tropopause height may vary if the static stability varies in response to a change in surface temperature. But baroclinic adjustment theories do predict a dependence of tropopause height on the tropospheric meridional temperature gradient, which depends in turn on the meridional temperature gradient at the surface. To test these predictions, two pairs of experiments were performed in which the lower boundary temperature (i.e., surface temperature over sea, deep soil temperature over land) was changed. In the first pair of experiments the lower boundary temperature was reduced uniformly by 10 K and by 20 K. In the second pair of experiments the equator to pole temperature gradient at the lower boundary was modified by adding $\pm(\sin^2\varphi)$ 20 K to the temperature. In all experiments the temperature changes were ramped in over the first 15 days.

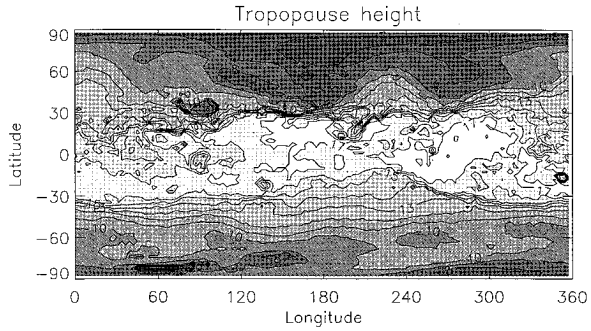

FIG. 3. Map of the tropopause height (km) on day 120 of the control integration.

As can be seen in Table 1, these experiments explicitly perturb all the parameters in (1), (4), and (5), with the exceptions of tropopause height and static stability, which are determined internally and are potentially subject to the radiative and dynamical constraints, and optical depth, which again is determined internally but is strongly influenced by the surface temperature. One further experiment was performed with perpetual July forcing.

3. Sensitivity to external parameters

Figure 3 shows a snapshot of the tropopause height on day 120 of the control integration, diagnosed according to the lapse rate definition. [Because of improvements to the radiation scheme and vertical advection scheme in the GCM, reducing noise in the vertical profile of temperature, we did not encounter the problems found by Juckes et al. (1994) in applying this definition of the tropopause in an earlier version of the UGAMP GCM.] The figure shows the general trend from a low tropopause at high latitudes to a high tropopause in the Tropics. A subtropical front is clearly visible in some regions as a sharp step in the tropopause height. However, there is no evidence of a sharp polar front. (The features near 85°S, 60°E and 30°N, 90°E are where the algorithm has misidentified a surface temperature inversion over high orography as the tropopause.) There is rather more small-scale variability in the Tropics than in the extratropics; this is probably related to the incidence of deep convection in the Tropics. The diagnostics presented below were all calculated for the last 30 days of the experiments described in section 2 from 18-hourly dumps of the model state. In a few cases diagnostics were also calculated for days 60 to 90 to confirm their robustness.

For each dump of the model state, the tropopause height was diagnosed as a function of longitude and latitude using the lapse rate criterion, then zonally averaged and time averaged. It is debatable whether the mean tropopause height calculated in this way is more relevant to the theories described in section 1 than the tropopause height diagnosed from the zonally averaged, time-averaged temperature. It has been verified for the control integration that the tropopause heights calculated in these two ways differ by less than 1 km almost everywhere, with the largest differences near the Tropics/extratropics transition. The 30-day mean, zonal mean tropopause height for nine of the ten experiments (the July run is excluded) is shown as a function of latitude ϕ in Fig. 4. The upper left panel shows the sensitivity of the tropopause height to changes in the ozone distribution. The tropopause height changes very little, perhaps by 1 km in the Tropics, when the ozone concentration profile is shifted downward by one scale height. When the ozone is removed completely, the temperature no longer increases with height in the stratosphere. However, the model continues to have a well-defined tropopause, only about 2 km higher than the control run in the Tropics and only about 1 km higher than the control run in the extratropics. In the extratropics, the tropopause remains quite sharp. The height of the tropopause is not strongly sensitive to the distribution of ozone, and indeed the presence of ozone is not essential to the existence of the tropopause. This is somewhat different from the results of Manabe and Strickler (1964), who found that in a radiative convective model under midlatitude conditions the tropopause became somewhat higher and much less marked when the radiative effects of ozone were removed. Note that the zonal mean time mean surface temperature in the runs with modified ozone distribution is virtually identical to that in the control run, because the sea surface temperature is specified and the soil temperature is strongly constrained, so the changes in tropopause height in these runs do not occur via changes in surface temperature.

The upper right panel shows the sensitivity of the tropopause height to changes in the earth's rotation rate. The tropical region is slightly narrower in the ''fast rotation'' run than in the ''slow rotation'' run. This reflects much larger latitudinal shifts in the jet maxima, which can be understood in terms of an angular momentum conserving Hadley circulation (Held and Hou 1980; Williams 1988). Apart from this, the tropopause height is virtually independent of changes in the earth's rotation rate. This is what would be predicted on the basis of (2) and (4). However, this insensitivity to rotation rate could also follow from other theories based on quasigeostrophic dynamics, so it cannot in itself be taken as confirmation of baroclinic adjustment theory.

The lower left panel shows the sensitivity of the tropopause height to globally uniform changes in the lower boundary temperature. The tropopause height is very sensitive to such changes. The tropopause moves downward about 5 km in the Tropics and about 2.5 km in the extratropics when the lower boundary temperature is reduced by 20 K. In the Tropics part of this sensitivity, but not all, can be explained by the fact that the moist adiabatic lapse rate is smaller in a warmer moister atmosphere than in a cooler drier atmosphere. In the ex-

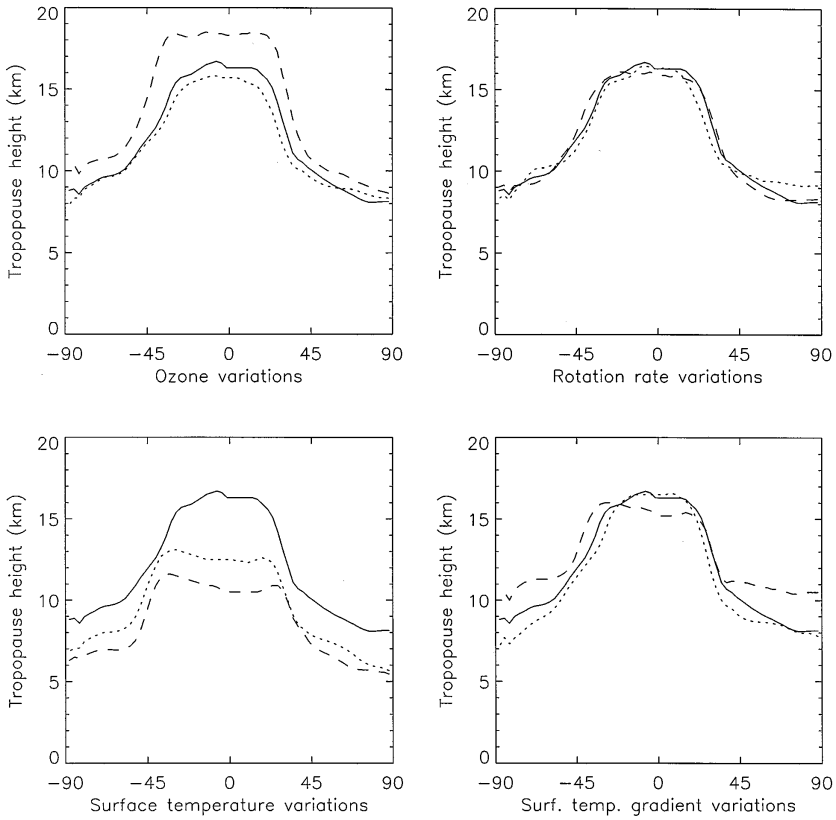

FIG. 4. Zonal mean 30-day mean tropopause height as a function of latitude for nine of the GCM experiments. In each panel the solid curve is for the control run, run 1. Upper left: dotted curve, run 2; dashed curve, run 3. Upper right: dotted curve, run 4; dashed curve, run 5. Lower left: dotted curve, run 6; dashed curve, run 7. Lower right: dotted curve, run 8; dashed curve, run 9.

tratropics this sensitivity would not be expected on the basis of baroclinic adjustment ideas, which depend on gradients of temperature rather than its absolute value. We shall see in the next section that a large part of this sensitivity to lower boundary temperature occurs through the dependence of atmospheric moisture on temperature and its resulting radiative effects.

The lower right panel of Fig. 4 shows the sensitivity of tropopause height to changes in the high-latitude lower boundary temperature while the equatorial temperature is kept fixed. Some baroclinic adjustment theories (e.g., Held 1982) suggest that the height of the extratropical tropopause should increase as the equator to pole temperature difference increases. The results presented here show that any such tendency is overwhelmed by the tendency for the tropopause height to increase as the surface temperature increases, so that the extratropical tropopause is highest in the ''warm pole'' run in which the equator to pole temperature gradient is smallest.

4. The radiative relationship

To investigate whether a simple radiative relationship indicated by (1) between γ and H holds in the UGAMP GCM, we have used the simple two-stream radiative transfer model of Goody (1964) as used by Held (1982) with two modifications described below. In this model absorption of solar radiation by the atmosphere is neglected. Let $\tau(z)$ be the optical depth measured from the top of the atmosphere, and let $U(\tau)$ and $D(\tau)$ be the upward and downward infrared irradiances and $B = \sigma T(\tau)^4$ where $\sigma = 5.67 \times 10^{-8}$ W m^{-2} K^{-4} is the Stefan–Boltzmann constant. Then

$$\frac{dU}{d\tau} = \frac{3}{2}(U - B), \tag{6}$$

$$\frac{dD}{d\tau} = \frac{3}{2}(B - D). \tag{7}$$

The boundary conditions are $U = \sigma T_*^4$ at $z = 0$, where T_* is the surface temperature, and $D = 0$ at $\tau = 0$. The troposphere is assumed to have a lapse rate γ while the stratosphere is assumed to be in radiative equilibrium. In the stratosphere, $U - D$ is a constant, denoted I, and this enables (6) and (7) to be integrated, giving

$$(U, D, B) = \left(1 + \frac{3\tau}{4}, \frac{3\tau}{4}, \frac{1}{2} + \frac{3\tau}{4}\right)I. \tag{8}$$

The most important difference from the model used by Held is the assumed profile of optical depth. Held specified a profile,

$$\tau(z) = \tau_* e^{-z/z_0}, \tag{9}$$

with the fixed values $z_0 = 2$ km and $\tau_* = 4.0$. In this paper we assume that τ is dominated by the water vapor distribution and that the relative humidity is approximately constant. Then τ can be parameterized by (9) with

$$\tau_* = 0.05 w_* z_0, \tag{10}$$

$$z_0 = 1/(0.07\gamma). \tag{11}$$

Here $w_*(T_*)$ is the water vapor saturation mass mixing ratio at the ground,

$$w_* = \frac{1}{p_0} 380.03 \exp\left[\frac{17.260(T_* - 273.16)}{(T_* - 35.86)}\right], \tag{12}$$

(Lowe 1977) with $p_0 = 10^5$ Pa. The coefficient 0.05 (dimensions of m^{-1}) in (10) accounts for many factors including the relative humidity and the optical properties of water vapor. The value 0.05 was chosen to give reasonable agreement between $H_{\rm RAD}$ predicted by this simple model and H from the GCM control integration over a range of middle latitudes. It implies $\tau_* \approx 0.059$ for $T_* = 250$ K and $\tau_* \approx 2.20$ for $T_* = 300$ K, which may be compared with the value $\tau_* = 4.0$ used by Held (1982). Having chosen this value of the coefficient, the same value was used for all subsequent calculations described here. The coefficient 0.07 (dimensions of K^{-1}) in (11) is an estimate of $(1/w_*)(\partial w_*/\partial T)$. The importance of including the parameterization (10) and (11) is discussed below.

There are several caveats concerning the optical depth profile given by (9), (10), and (11). The longwave effects of carbon dioxide and ozone have been neglected, and the water vapor is assumed to continue to fall off rapidly with height in the stratosphere. As a result, the formula gives unrealistically small values of optical depth both in the stratosphere and in the high latitudes of the troposphere. It turns out, however, that the calculation of $H_{\rm RAD}$ is not sensitive to the exact details of the τ profiles in these regions provided that they are optically thin. Similarly, the assumption of constant relative humidity is a gross simplification. However, variations in τ_* are dominated by variations in temperature rather than variations in the relative humidity. For example, a change of, say, 20% in the relative humidity for a given temperature profile would correspond to a change of 20% in τ_*, whereas a change in the temperature of 10 K for a given relative humidity would correspond to a change in τ_* of roughly a factor of 2. Another factor that has been neglected is the effect of clouds. This is likely to be especially important in the Tropics where there are large amounts of high, and therefore cold, optically thick clouds. It is probable that the choice of the coefficient in (10) compensates to some extent for some of these simplifications.

The second, more minor, difference from the model used by Held is that Held determined T_* iteratively by the requirement that the outgoing infrared flux at the top of the atmosphere should balance some implied heating of the ground and the troposphere. Here we take T_* to be specified. This is more consistent with the GCM, in which sea surface and deep soil temperatures are specified. It should also be a reasonable approximation for the real world for timescales of a few weeks over which the tropopause height responds to changes in forcing but sea surface temperatures change little. It turns out that this formulation simplifies the calculation of the tropopause height for a given tropospheric lapse rate. Given T_* and γ, the tropospheric temperature and hence B are easily calculated, and then U can be found by integrating (6) up from the lower boundary. At the lower boundary $U = B$, but B decreases more rapidly with height than U. At some level, $z = H_{\rm RAD}$, the condition $U/B = (1 + 3\tau/4)/(1/2 + 3\tau/4)$ is satisfied; from this level upward the radiative equilibrium profile (8) is possible. Therefore $H_{\rm RAD}$ is identified with the tropopause height. Thus, with fixed T_*, $H_{\rm RAD}$ can be found with a single integration through the column, without the need for iteration.

Figure 5 shows the importance of including the dependence of moisture on temperature in this calculation. Figure 5a shows $H_{\rm RAD}(T_*, \gamma)$ calculated using the optical depth profile (9) with $z_0 = 2$ km and $\tau_* = 4.0$. This suggests that over the range of T_* and γ found in the present climate, the tropopause height will be more sensitive to tropospheric lapse rate than to surface temperature. Figure 5b shows $H_{\rm RAD}(T_*, \gamma)$ calculated using (9) with z_0 and τ_* given by (10) and (11). When the dependence of moisture on temperature is included, the sensitivity to T_* is greatly increased.

Figure 6 shows $H_{\rm RAD}(T_*, \gamma)$, calculated using zonal mean $T_*(\phi)$ and $\gamma(\phi)$ taken from the GCM, plotted against zonal mean $H(\phi)$ taken directly from the GCM. A vertically averaged value of γ is estimated as $-(\overline{T}_{TP} - \overline{T}_N)/H$, where $\overline{T}_{TP}$ is the zonal mean of the temperature at the tropopause, $\overline{T}_N$ is the zonal mean of the temperature at the lowest model level, and H is the zonal mean of the tropopause height. Data for all ten integrations are included but data from the Tropics ($|\phi| < 30°$) and data poleward of 60° in the winter hemisphere are excluded, leaving 31 data points per integration. For the latitudes shown, $H_{\rm RAD}$ agrees remarkably well with H. This agreement occurs not just at a single point in parameter space but over a range of H values, a range of latitudes, and a range of other conditions. The dependence of H on T_* and, to some extent, on γ predicted by the radiative relationship has been well verified.

Note that the variations in water vapor content with

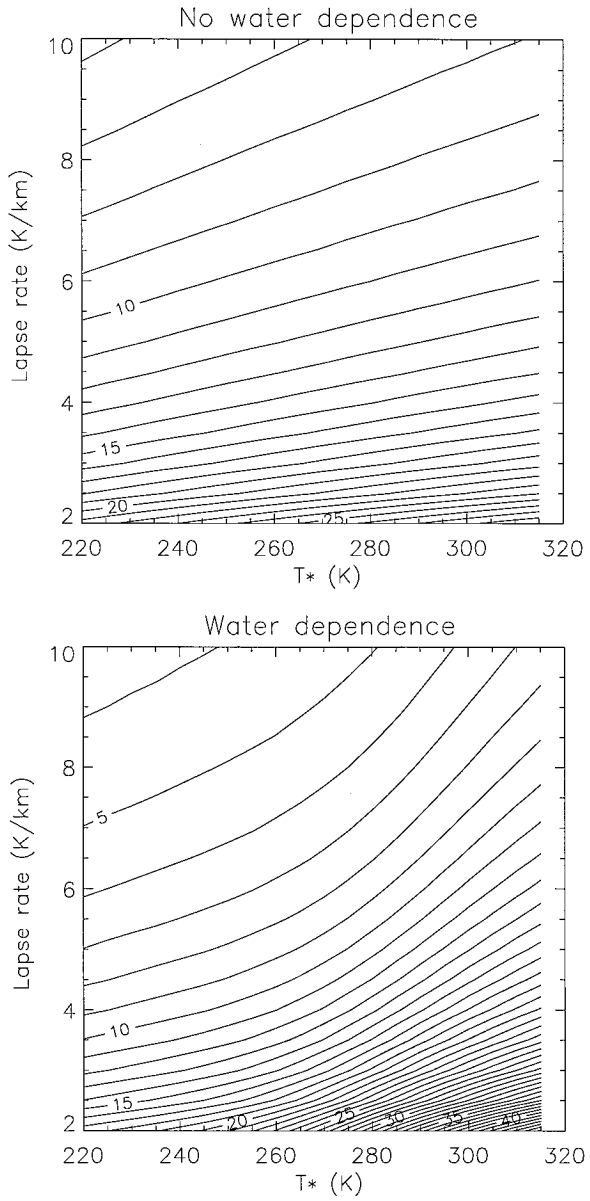

FIG. 5. Tropopause height (km) as a function of temperature (K) and lapse rate (K km^{-1}) predicted by the simple radiative model. (a) Using the optical depth profile (9) with $\tau_* = 4.0$ and $z_0 = 2$ km. (b) Using (9) with τ_* and z_0 given by (10) and (11).

temperature given by (10) and (11) are crucial for capturing the dependence of H_{RAD} on T_*. When the calculation is repeated using $\tau_* = 4.0$ and $z_0 = 2$ km, the slope of the resulting H_{RAD} versus H plot (not shown) is close to 0.5 rather than 1. Interestingly, a similar difference in sensitivity was found by Manabe and Wetherald (1967), who showed that the sensitivity of the equilibrium surface temperature to changes in various radiative forcing factors in a radiative convective model was approximately twice as great for a given

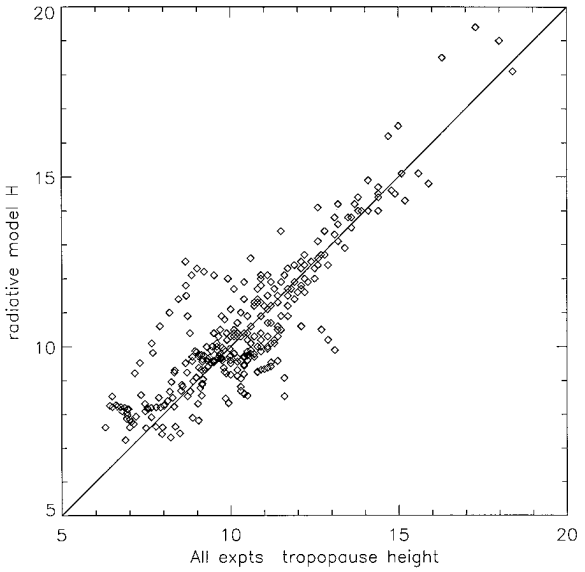

FIG. 6. H_{RAD} (km) vs H (km). Data for all ten integrations are included but data from the Tropics ($|\phi| < 30°$) and data poleward of 60° in the winter hemisphere are excluded.

distribution of relative humidity as for a given distribution of absolute humidity.

Figure 7 shows $H_{\mathrm{RAD}}(T_*, \gamma)$ plotted against H for all latitudes of the control integration. There are clear deviations from the radiative model prediction in the Tropics, where H_{RAD} is significantly less than H, and near the winter pole, where H_{RAD} is significantly greater than H. The other integrations show a similar pattern.

There are several possible explanations for the disagreement between H_{RAD} and H near the winter pole.

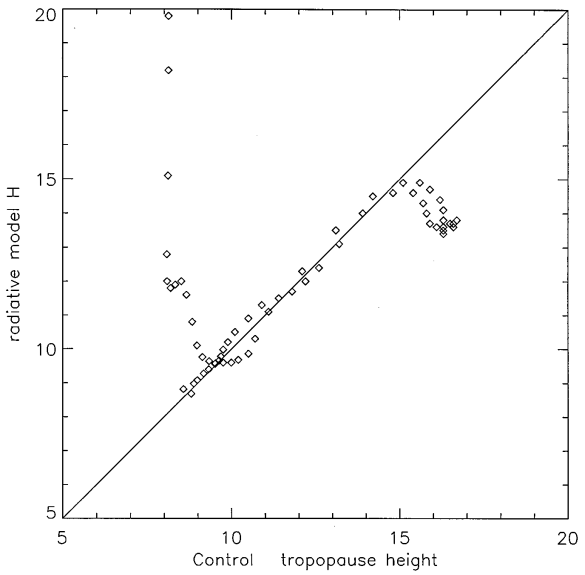

FIG. 7. H_{RAD} (km) vs H (km) for all latitudes of the control integration.

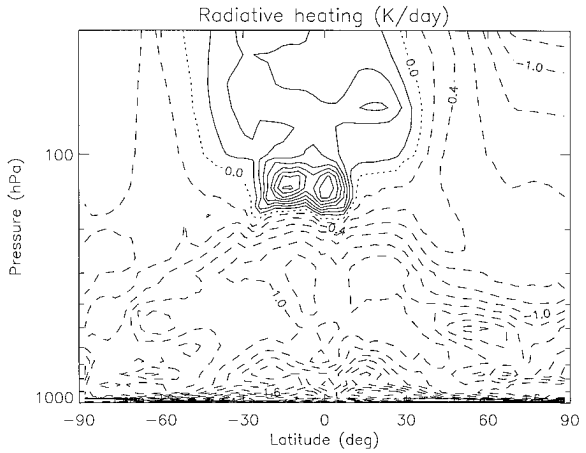

FIG. 8. Zonal mean net radiative heating rate (K day^{-1}) as a function of latitude and approximate pressure (hPa) averaged over days 90.75–120.0 of the control integration. The zero contour is dotted and negative contours are dashed.

One is that there may not be a sharp, well-defined tropopause in the GCM at these latitudes. However, individual temperature profiles from the GCM show that a fairly sharp, well-defined tropopause does indeed exist. A second possible explanation is that wave-driven descent in the winter stratosphere is strong enough to imply temperatures significantly warmer than radiative equilibrium there, so that the assumptions used in calculating $H_{\mathrm{RAD}}(T_*, \gamma)$ are not valid. The radiative heating rate in the GCM (Fig. 8) does indeed show values around -0.5 K day^{-1} just above the tropopause near the winter pole, slightly larger in magnitude than in other regions of the extratropical lower stratosphere. However, a more important factor is the strong temperature inversion that forms next to the ground at high latitudes in the winter, with T increasing by 10–20 K between 1000 hPa and about 900 hPa. This means that the average lapse rate as we have diagnosed it between the lowest model level and the tropopause is rather low, maybe 3–4 K km^{-1} or lower. Indeed, a lapse rate this small is the only way that such large values of H_{RAD} can be obtained, given the cold surface temperatures at these latitudes (see Fig. 5b). However, the tropospheric lapse rate above the temperature inversion is typically 5–6 K km^{-1}. The implication is that, for the purpose of calculating H_{RAD}, a temperature structure like this cannot be characterized by a simple depth-average lapse rate.

It is perhaps surprising that H_{RAD} disagrees with H in the Tropics where it is often assumed that the mechanisms determining the tropopause height are well understood. However, the simple picture of a stratosphere close to radiative equilibrium above a convectively adjusted troposphere is an oversimplification. To begin with, the zonal mean tropopause height in the control integration according to the lapse rate criterion is about 16.5 km (100 hPa), whereas the minimum of the zonal mean temperature occurs at about 18 km (80 hPa). However, the peak in the winterward branch of the Hadley circulation occurs much lower down, at around 13.5 km (160 hPa). Convection statistics from the control GCM integration and cloud top temperatures estimated from outgoing longwave radiation data for the real world both suggest that the great majority of convection reaches no higher than about 150 hPa, with only a small fraction reaching the tropopause (E. J. Highwood 1995, personal communication). The tropical tropopause appears to coincide with the highest level reached by convection, as claimed by Schneider (1977), but the points just noted suggest that only that part of the tropical troposphere below about 150 hPa is maintained close to a moist adiabat by convection. A similar suggestion has been made by Sinha and Shine (1994), based on the results of a one-dimensional radiative–convective model in which the temperature minimum occurred in a region in purely radiative equilibrium, well above the convectively adjusted region. Certainly, the saturation equivalent potential temperature θ_{e*} from the control GCM integration shows values increasing significantly in the uppermost tropical troposphere. In some individual column temperature profiles from the Tropics of the GCM, though not all, a clear change in slope is visible at some level between 200 hPa and 100 hPa. This may be the GCM analog of the secondary ''thermal'' tropopause identified by Shapiro et al. (1982) at around 12 km in the Tropics.

One feature of the GCM integration that complicates the interpretation of the results in the tropical upper troposphere is that the Betts–Miller convection scheme produces a significant *cooling* between 150 hPa and 100 hPa, peaking at about 1.4 K day^{-1} in the zonal mean. (This is despite the relatively small number of cumulus clouds reaching these levels.) This is compensated mainly by radiative heating (Fig. 8). The convective cooling arises because the reference temperature profile, toward which the model temperature profile is adjusted, is modified to enforce approximate conservation of the column integrated enthalpy. Although this convective cooling is unrealistic, it may have a real-world counterpart in that convective turrets overshooting their level of neutral buoyancy will tend to cool the environment as they detrain. Note that here we are referring to turrets overshooting their level of neutral buoyancy well below the tropopause, not overshooting the tropopause itself. Indeed, such cooling by overshooting turrets provides a possible mechanism for sharpening the tropopause. Figure 8 also shows significant radiative heating extending through the tropical tropopause and well up into the tropical stratosphere. Indeed, the radiative heating between 150 hPa and 100 hPa is more than enough to compensate for convective cooling. Examination of the heat budget confirms that the net diabatic heating is balanced by adiabatic cooling associated with ascent—part of the same wave-driven global stratospheric circulation that leads to descent and temperatures above radiative equilibrium in the winter polar stratosphere.

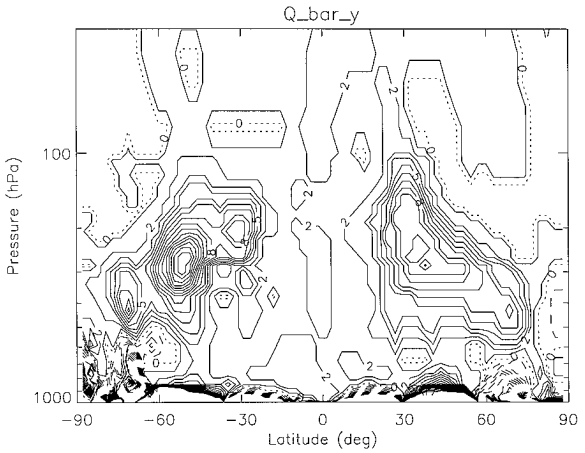

FIG. 9. Zonal mean $\bar{q}_y$ (s^{-1} m^{-1}) as a function of latitude and approximate pressure (hPa) averaged over days 90.75–120.0 of the control integration. The contour interval is 10^{-11} s^{-1} m^{-1}. The zero contour is dotted and negative contours are dashed.

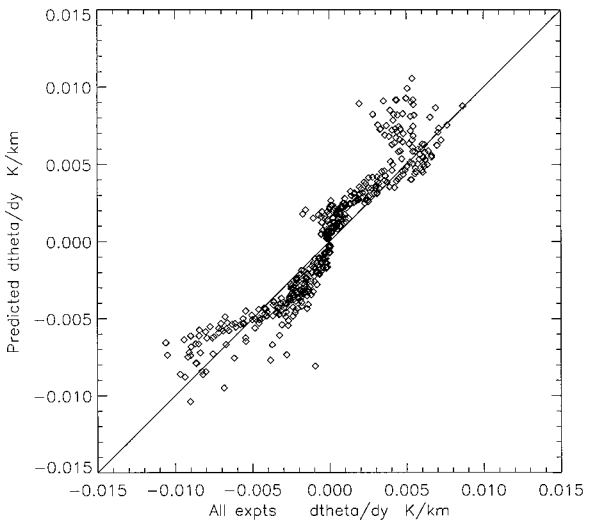

FIG. 10. Plot of $\bar{\theta}_y$ predicted by the other parameters in (4) vs $\bar{\theta}_y$ taken directly from the GCM. Data for latitudes greater than 30° from all ten experiments are shown.

5. Baroclinic adjustment

This section examines the extent to which some of the predictions of baroclinic adjustment theory discussed in section 1 hold in our GCM integrations. We first consider the extent to which the atmosphere satisfies the condition that in the extratropics $\bar{\theta}_y$ near the ground and $\bar{q}_y$ over some depth of the troposphere should vanish. In our GCM integrations, $\bar{\theta}_y$ near the ground in the extratropics does not vanish. An appropriate measure of the smallness of $\bar{\theta}_y$ is the Eady growth rate $\sigma = 0.31|(f/N)u_z| \approx 0.31(g/N)|\bar{\theta}_y/\bar{\theta}|$ (Lindzen and Farrell 1980a). Typical values for the extratropics are around 1.5 day^{-1}, which is certainly not small compared to the reciprocals of the other timescales involved.

Figure 9 shows $\bar{q}_y$ averaged over the last 30 days of the control integration. The large gradients in the region of the extratropical tropopause are clearly visible, despite some smoothing by time averaging and zonal averaging. However, it is not clear that the tropospheric values are small enough (compared with β) to be regarded as effectively zero. Similarly, isentropic maps of Rossby–Ertel PV show small values and small gradients in the troposphere, but again it is not clear whether the gradients are small enough (compared, for example, with $g\beta$ times a mean value of $\partial\theta/\partial p$ over the isentrope) to be regarded as effectively zero. A more rigorous test is required.

We next attempted to test the scaling implied by (4) by examining whether the parameters varied together in the predicted way. One problem with this approach is that the height scale $H_{(s)}$ has no simple interpretation. Figure 10 shows a scatterplot of the predicted $\bar{\theta}_y = -\bar{\theta}_z H_{(s)}\beta/f$ against the actual $\bar{\theta}_y$ from the GCM, where $H_{(s)}$ takes the constant value 7000 m and $\bar{\theta}_z$ is a tropospheric depth average taken from the GCM. Here, $\bar{\theta}_y$ from the GCM has been calculated on a model level close to 600 hPa. There is a region near the center of the scatter plot where the predicted $\bar{\theta}_y$ agrees well with the actual $\bar{\theta}_y$. These are points on the poleward sides of the jet maxima. A similar agreement was found by Stone (1978). However, this agreement may be associated principally with a correlation between $\bar{\theta}_y$ and β/f, since both are constrained by spherical geometry to go smoothly to zero at the pole, while $H_{(s)}$ and $\bar{\theta}_z$ remain finite and nonzero. The degree of agreement remains similar when $H_{(s)}$ is replaced by the tropopause height.

A more stringent test of baroclinic adjustment using the same data is to calculate the value of $H_{(s)}$ implied by the other parameters in (4). Since this formula involves only the ratio of $\bar{\theta}_y$ and β/f, it is not constrained by their behavior near the pole. For (4) to be useful, $H_{(s)}$ must either be an empirical constant or be related to some measurable quantity like the tropopause height. A scatter plot of $H_{(s)}$ calculated from (4) shows that it is neither approximately constant nor related to the tropopause height, even when attention is restricted to a narrow band of latitudes ($30° < |\phi| < 60°$) over which baroclinic waves are most active (Fig. 11). There is no evidence even for the ''weak'' version of baroclinic adjustment (Stone and Branscome 1992).

A final way of looking at the same data is to compare $\bar{\theta}_z$ predicted by (4) (taking $H_{(s)}$ = 7000 m) with $\bar{\theta}_z$, averaged over the depth of the troposphere, taken directly from the GCM (Fig. 12). Points poleward of 60° in the winter hemisphere have been omitted because $\bar{\theta}_z$ as diagnosed from the GCM was not typical of the free troposphere, as discussed in section 4. As expected from the results already discussed, the predicted and model values of $\bar{\theta}_z$ do not agree. However, there is far more scatter in the predicted $\bar{\theta}_z$ than in the actual $\bar{\theta}_z$; the actual $\bar{\theta}_z$ values are clustered close to 5 K km^{-1}. The exceptional points, where the actual $\bar{\theta}_z$ value is low, occur in

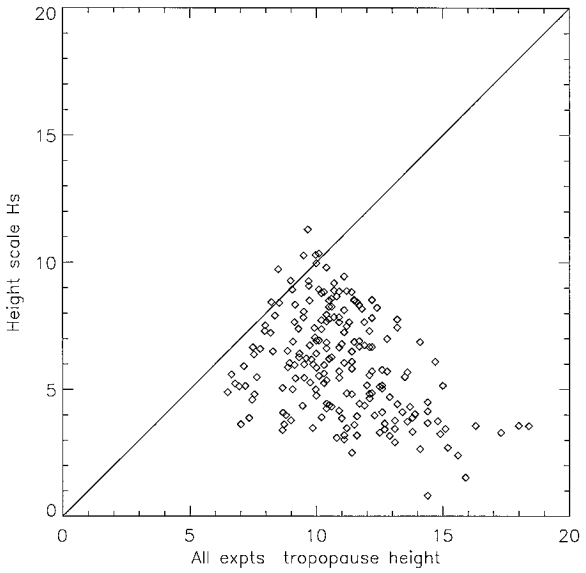

FIG. 11. Plot of $H_{(s)}$ predicted by the other parameters in (4) vs H taken directly from the GCM. Data from the latitude bands $30° < |\phi| < 60°$ for all ten experiments are shown.

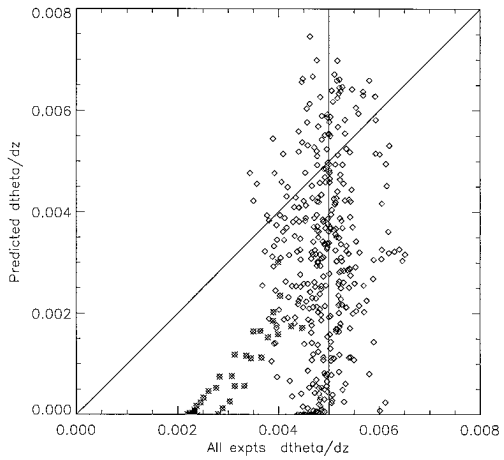

FIG. 12. Plot of $\bar{\theta}_z$ predicted by the other parameters in (4) vs $\bar{\theta}_z$ taken directly from the GCM. Data from all ten experiments are shown but points poleward of 60° in the winter hemisphere are omitted. Points from the Tropics ($|\phi| < 30°$) of runs 6 and 7 are shown by diamonds overplotted with crosses.

the Tropics of the runs with uniformly reduced surface temperature. In these runs the atmosphere is much colder and drier than in the control run so that the convectively adjusted state in the Tropics is much closer to a dry adiabat. However, the extratropical lapse rate in these runs does not appear to be greatly influenced by the dramatic changes in the tropical lapse rate.

Next we examined the relationship (5) implied by baroclinic neutrality with respect to Eady modes. Here, $K_{\max}$ is readily calculated using N^2 and H from the GCM. For convenience, $K_{\max}$ was reexpressed as an equivalent planetary zonal wavenumber $m_{\max}$ by writing $K^2_{\max} = k^2 + l^2$; $k = l$; $m_{\max} = ka\cos\phi$, where a is the earth's radius. It has been assumed that the zonal and meridional scales of the eddies are the same, but the conclusions below would not be affected by other reasonable assumptions about the eddies' shape. Figure 13 shows $m_{\max}$ as a function of latitude for nine of the ten GCM runs.

The upper right panel shows that $m_{\max}$ increases as f increases from one experiment to another. There is no compensation between f and N or H on the right-hand side of (5). But the width of the jet does decrease by a factor of about 2 between the slow rotation run and the fast rotation run, so in this case $m_{\max}$ does scale like the inverse of the jet width, and this is consistent with Lindzen's conjecture. However, the upper left and lower left panels of Fig. 13 show that $m_{\max}$ at a given latitude varies inversely as the tropopause height in cases where the jet width does not change appreciably. The compensation between N and H required to satisfy (5) does not occur. Therefore these results are not consistent with Lindzen's conjecture.

Incidentally, (5) can be put into a form resembling (4), but with the tropopause height H replacing the height scale $H_{(s)}$, if we assume that the jet width is given by the Rhines (1975) β-scale $K^2_{\min} \approx \beta/\bar{u}$ and that $\bar{u}/H$ is given by thermal wind balance, $\bar{u}/H \approx -\bar{\theta}_y/(gf\theta)$. However, the relationship (4) has already been shown not to hold across all our experiments.

6. Summary

The sensitivity of the tropopause height to various external parameters has been investigated using a GCM in perpetual January mode. The tropopause height was found to be strongly sensitive to the temperature at the earth's surface through changes in the moisture distribution and its resulting radiative effects. The tropopause height is less sensitive to changes in the ozone distribution and hardly sensitive at all to moderate changes in the earth's rotation rate.

The assumption that the lower stratosphere is close to radiative equilibrium leads to a relationship between tropospheric lapse rate, surface temperature, and tropopause height. Variations in the moisture distribution have a big effect on this relationship. A simple parameterization of the moisture distribution in terms of the surface temperature and the lapse rate has been used to take this into account. With this parameterization, this radiative relationship was found to hold well in the GCM experiments in the extratropics away from the winter pole. It is likely that H_{RAD} could be made to agree with H near the winter pole too by specifying the temperature profile up to the top of the inversion as well as the free tropospheric lapse rate. In the Tropics, several factors lead to the breakdown of the radiative relationship. One of these is that only that part of the tropical troposphere below about 13.5 km can be regarded as dominated by convective adjustment; between this level

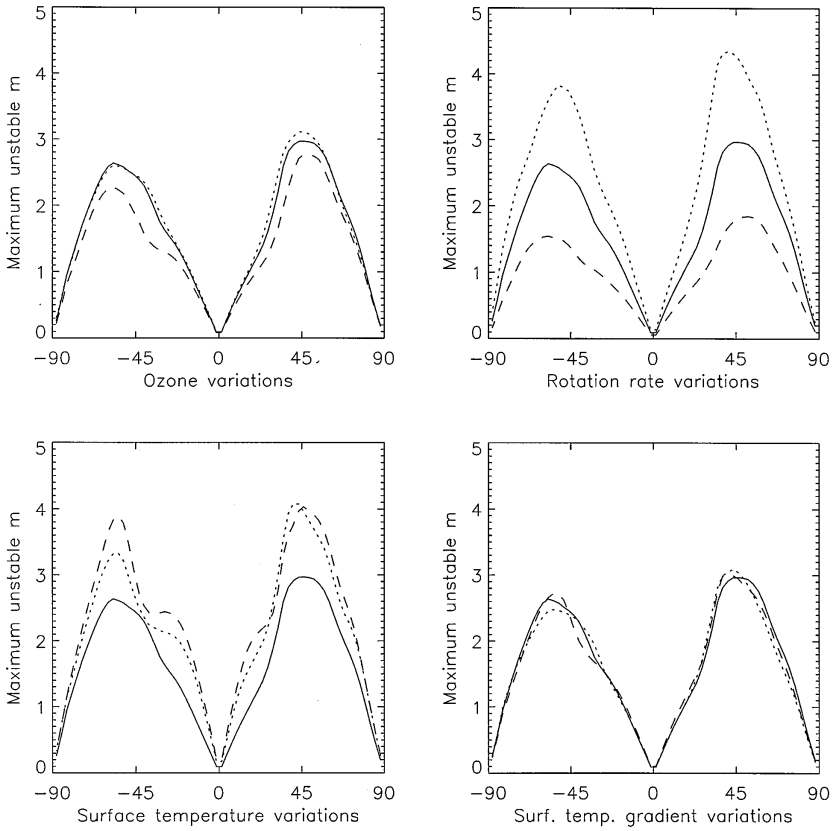

FIG. 13. Plots of m_{max} as a function of latitude for nine of the ten GCM experiments. In each panel the solid curve is for the control run, run 1. Upper left: dotted curve, run 2; dashed curve, run 3. Upper right: dotted curve, run 4; dashed curve, run 5. Lower left: dotted curve, run 6; dashed curve, run 7. Lower right: dotted curve, run 8; dashed curve, run 9.

and the tropopause convection, radiation, and large-scale upwelling all play a role.

Two versions of baroclinic adjustment have been investigated in the GCM. The first is based on the Charney–Stern sufficient condition for stability of quasi-geostrophic flow and leads to the relation (4). The second is based on neutrality with respect to Eady modes and leads to the relation (5). Both of these relations hold approximately when typical values of the parameters are inserted. However, when specifiable parameters are changed in our GCM experiments the remaining parameters do not respond in the predicted way: the height scale $H_{(s)}$ calculated from the other terms in (4) appears to have virtually no correlation with the tropopause height, nor is it a constant; and the tropopause height can vary in response to surface temperature changes while the other terms in (5) remain unchanged. These results cast doubt on the relevance of baroclinic adjustment to the height of tropopause.

One intriguing aspect of our experiments is that the lapse rate in the extratropical free troposphere varies much less than predicted by the baroclinic adjustment theories in response to the imposed changes in other parameters. This suggests that the extratropical lapse rate may be effectively fixed by some mechanism other than those we have considered. This mechanism, if it exists, does not appear to tie the extratropical lapse rate closely to the tropical lapse rate, as is shown by the runs with colder lower boundary, in which the tropical and extratropical lapse rates are significantly different. A focus for future work will be to investigate possible mechanisms controlling the extratropical lapse rate.

Acknowledgments. We would like to thank E. J. Highwood, B. J. Hoskins, K. P. Shine, and A. J. Thorpe for many stimulating discussions and careful comments on an earlier version of this paper. JT was supported by the U.K. Natural Environment Research Council through the U.K. Universities Global Atmospheric Modelling Programme.

REFERENCES

Betts, A. K., and M. J. Miller, 1994: The Betts–Miller scheme. *The Representation of Cumulus Convection in Numerical Models of the Atmosphere, Meteor. Monogr.* No. 46, K. A. Emanuel and D. J. Raymond, Eds., Amer. Meteor. Soc., 107–121.

Charney, J. G., and M. E. Stern, 1962: On the stability of internal

baroclinic jets in a rotating atmosphere. *J. Atmos. Sci.,* **19,** 159–172.
Eady, E. T., 1949: Long waves and cyclone waves. *Tellus,* **1,** 33–52.
Egger, J., 1995: Tropopause height in baroclinic channel flow. *J. Atmos. Sci.,* **52,** 2232–2241.
Goody, R. M., 1964: *Atmospheric Radiation.* Vol. I, *Theoretical Basis,* Clarendon Press, 436 pp.
Gutowski, W. J., 1985: Baroclinic adjustment and midlatitude temperature profiles. *J. Atmos. Sci.,* **42,** 1733–1745.
Held, I. M., 1982: On the height of the tropopause and the static stability of the troposphere. *J. Atmos. Sci.,* **39,** 412–417.
——, and A. Y. Hou, 1980: Nonlinear axially symmetric circulations in a nearly inviscid atmosphere. *J. Atmos. Sci.,* **37,** 515–533.
Hoerling, M. P., T. K. Shaack, and A. J. Lenzen, 1991: Global objective tropopause analysis. *Mon. Wea. Rev.,* **119,** 1816–1831.
Holton, J. R., P. H. Haynes, M. E. McIntyre, A. R. Douglass, R. B. Rood, and L. Pfister, 1995: Stratosphere–troposphere exchange. *Rev. Geophys.,* **33,** 403–439.
Houghton, J. T., 1977: *The Physics of Atmospheres.* Cambridge University Press, 203 pp.
Juckes, M. N., I. N. James, and M. Blackburn, 1994: The influence of Antarctica on the momentum budget of the southern extratropics. *Quart. J. Roy. Meteor. Soc.,* **120,** 1017–1044.
Lait, L. R., 1994: An alternative form for potential vorticity. *J. Atmos. Sci.,* **51,** 1754–1759.
Leonard, B. P., 1991: The ULTIMATE conservative difference scheme applied to unsteady one-dimensional advection. *Comput. Methods Appl. Mech. Eng.,* **88,** 17–74.
Lewis, R. P. W., Ed., 1991: *Meteorological Glossary.* 6th ed. Her Majesty's Stationer's Office, 335 pp.
Lindzen, R. S., 1993: Baroclinic neutrality and the tropopause. *J. Atmos. Sci.,* **50,** 1148–1151.
——, and B. Farrell, 1980a: A simple approximate result for maximum growth rate of baroclinic instabilities. *J. Atmos. Sci.,* **37,** 1648–1654.
——, and ——, 1980b: The role of the polar regions in global climate, and a new parameterization of global heat transport. *Mon. Wea. Rev.,* **108,** 2064–2079.
Lowe, P. R., 1977: An approximating polynomial for the computation of saturation vapor pressure. *J. Appl. Meteor.,* **16,** 100–103.
Manabe, S., and R. F. Strickler, 1964: Thermal equilibrium of the atmosphere with a convective adjustment. *J. Atmos. Sci.,* **21,** 361–385.
——, and R. T. Wetherald, 1967: Thermal equilibrium of the atmosphere with a given distribution of relative humidity. *J. Atmos. Sci.,* **24,** 241–259.
McIntyre, M. E., and T. N. Palmer, 1984: The 'surf zone' in the stratosphere. *J. Atmos. Terr. Phys.,* **46,** 825–849.
Morcrette, J.-J., 1990: Impact of changes to the radiation transfer parametrizations plus cloud optical properties in the ECMWF model. *Mon. Wea. Rev.,* **118,** 847–873.
Palmén, E., and C. W. Newton, 1969: *Atmospheric Circulation Systems: Their Structure and Physical Interpretation.* International Geophysical Series, Vol. 13, Academic Press, 603 pp.
Phillips, N. A., 1954: Energy transformations and meridional circulations associated with simple baroclinic waves in a two-level, quasi-geostrophic model. *Tellus,* **6,** 273–286.
Rhines, P., 1975: Waves and turbulence on a β-plane. *J. Fluid Mech.,* **69,** 417–443.
Schneider, E. K., 1977: Axially symmetric steady-state models of the basic state for instability and climate studies. Part II. Nonlinear calculations. *J. Atmos. Sci.,* **34,** 280–296.
Shapiro, M. A., A. J. Krueger, and P. J. Kennedy, 1982: Nowcasting the position and intensity of jet streams using a satellite-based total ozone mapping spectrometer. *Nowcasting,* K. A. Browning, Ed., Academic Press, 137–145.
——, T. Hampel, and A. J. Krueger, 1987: The arctic tropopause fold. *Mon. Wea. Rev.,* **115,** 444–454.
Shine, K. P., 1989: Sources and sinks of zonal momentum in the middle atmosphere diagnosed using the diabatic circulation. *Quart. J. Roy. Meteor. Soc.,* **115,** 265–292.
Sinha, A., and K. P. Shine, 1994: A one-dimensional study of possible cirrus cloud feedbacks. *J. Climate,* **7,** 158–173.
Slingo, J., M. Blackburn, A. K. Betts, R. Brugge, K. Hodges, B. J. Hoskins, M. J. Miller, L. Steenman-Clark, and J. Thuburn, 1994: Mean climate and transience in the Tropics of the UGAMP GCM: Sensitivity to convective parametrization. *Quart. J. Roy. Meteor. Soc.,* **120,** 881–922.
Stone, P. H., 1978: Baroclinic adjustment. *J. Atmos. Sci.,* **35,** 561–571.
——, and J. H. Carlson, 1979: Atmospheric lapse rate regimes and their parameterization. *J. Atmos. Sci.,* **36,** 415–423.
——, and L. Branscome, 1992: Diabatically forced, nearly inviscid eddy regimes. *J. Atmos. Sci.,* **49,** 355–367.
Sun, D.-Z., and R. S. Lindzen, 1994: A PV view of the zonal mean distribution of temperature and wind in the extratropical troposphere. *J. Atmos. Sci.,* **51,** 757–772.
Valdes, P. J., and B. J. Hoskins, 1988: Baroclinic instability of the zonally averaged flow with boundary layer damping. *J. Atmos. Sci.,* **45,** 1584–1593.
Vallis, G. K., 1988: Numerical studies of eddy transport properties in eddy-resolving and parametrized models. *Quart. J. Roy. Meteor. Soc.,* **114,** 183–204.
Williams, G. P., 1988: The dynamical range of global circulations—I. *Climate Dyn.,* **2,** 205–260.
——, and J. L. Holloway, 1982: The range and unity of planetary circulations. *Nature,* **297,** 295–299.